

The chemical structure of bipolar planetary nebulae[★]

II. 13 objects

Mario Perinotto¹ and Romano L.M. Corradi²

¹ Dipartimento di Astronomia e Scienza dello Spazio, Università di Firenze, Largo E. Fermi 5, I-50125 Firenze, Italy

² Instituto de Astrofísica de Canarias, c. Via Lactea S/N, E-38200 La Laguna, Tenerife, Spain

Received 12 June 1997 / Accepted 24 December 1997

Abstract. Long slit spectrophotometry of 13 bipolar planetary nebulae has been used to study their physical and chemical properties. In each nebula, one to seven different spatial regions have been considered in order to search for possible abundance variations through the nebulae. We obtained the following main results:

– within the errors, the He, O, and N abundances are constant through all the nebulae.

– the Ne, Ar, and S abundances are also constant, within the errors, but their face values have systematic increases toward the outer regions of the nebulae. These trends may be attributed to inaccuracies in the ionization correction factors, as predicted by Alexander & Balick (1997) for long-slit observations of extended PNe. The corresponding increase of the N abundance predicted by those authors is, however, generally not observed (with one exception).

– The present sample contains some of the Galactic PNe with the highest He and N/O abundances known to date (M 3–2, He 2–111, NGC 6537). The highest He overabundances cannot be reproduced by any current model of AGB evolution.

– Oxygen depletion is suggested for the nebulae with the highest N/O abundances, indicating that efficient ON cycle process has occurred in their progenitors¹.

Key words: ISM: abundances – planetary nebulae: general

1. Introduction

The morphological appearance of planetary nebulae (PNe) has since long attracted the attention of the researchers. Various designations and/or classification schemes have then been proposed since the early work of Curtis (1918) up to the most recent ones (Balick 1987, Schwarz et al. 1993, Machado et al. 1996). Particularly significant for the implications with the evolutionary history of PNe has been the recognition of the close

Send offprint requests to: R. Corradi (rcorradi@iac.es)

[★] Based on observations made at the European Southern Observatory

¹ Tables 4 to 29 are only available in electronic form at the CDS via anonymous ftp to cdsarc.u-strasbg.fr (130.79.128.5) or via <http://cdsweb.u-strasbg.fr/Abstract.html>

Table 1. Log of the observations.

| Object | Exp. tim. [min] | range [nm] | P.A. [deg] | Notes [†] |
|----------|--------------------|---------------|---------------|--------------------|
| NGC 2440 | 1,2,30,30 (2, 40) | 360–960 | +83 | |
| NGC 2818 | 2,40 | 360–710 | +80 | |
| NGC 2899 | 2,40 | 360–710 | +25 | short axis |
| NGC 6072 | 2,55 | 360–710 | +67 | |
| NGC 6537 | 2,8,20,60 (2,60) | 360–960 | +18 | |
| He 2–36 | 2,40 | 360–710 | –41 | |
| He 2–84 | 1,40 (2,45) | 360–960 | +30 | |
| He 2–111 | 40 | 360–710 | +10 | short axis |
| He 2–114 | 40 | 360–710 | +89 | short axis |
| M 1–13 | 2,40 | 360–710 | –29 | |
| M 1–16 | 2,40 | 360–710 | –26 | |
| M 3–2 | 2,40 | 360–710 | –45 | short axis |
| Mz 1 | 5,38 | 360–960 | –26 | |

[†]Unless indicated, the slit position is approximately along the symmetry axis of the bipolar nebula (see Fig. 1). Within parentheses, the exposure times in the near-IR spectra (710–960 nm).

correlation between the enhanced chemical abundances in He/H and/or N/O (Peimbert, 1978) and the bipolar morphology of the nebula. This as well as other properties of this class, including the properties of the central stars and their galactic location, was extensively investigated by several authors (see Corradi & Schwarz 1995, hereafter CS95, for a recent comprehensive study). Nearly all bipolar PNe belong in fact to type I PNe (Peimbert, 1978; Peimbert & Torres–Peimbert 1983) defined by having either $\text{He}/\text{H} \gtrsim 0.125$ or $\log(\text{N}/\text{O}) \gtrsim -0.3$. These overabundances have been related to more massive progenitors for the central stars of these PNe, as compared with those of PNe of other morphological classes. Massive AGB stars ($M_i \gtrsim 2 M_{\odot}$) are in fact expected to be substantially He and/or N enriched at their surface, following second and third dredge-up episodes as well as efficient H–burning at the base of the convective envelope (Renzini & Voli 1981). Recent calculations (Marigo et al. 1996, and 1997, private communication) fail, however, to reproduce the most extreme He overabundances measured in some bipolar PNe.

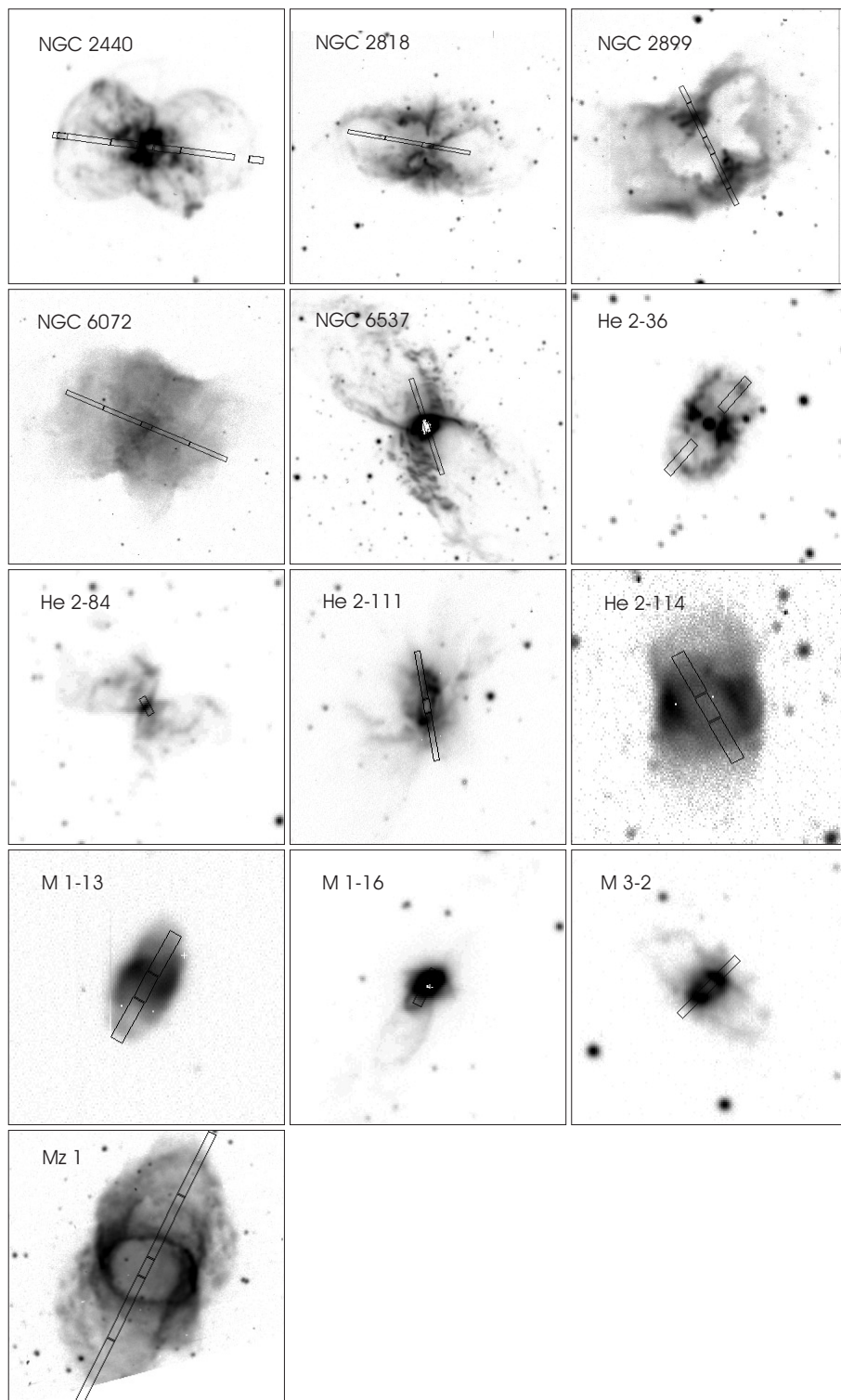


Fig. 1. The $H\alpha$ + $[NII]$ images of the nebulae; a drawing of the adopted slit position is superimposed on the images. North is at the top, East to the left. Slits are split in order to show the regions from which average 1–D spectra were extracted (see text). Images are from CS95.

In order to better quantify these problems, we have obtained deep long-slit spectra of fourteen bipolar nebulae selected from the compilation of CS95. From these data, we have derived new, homogeneous, good quality chemical abundances. By means of these observations, we also wished to investigate the possibility of detecting chemical variations through the nebulae, which may reflect different mass loss episodes from their progenitors,

or be the trace of chemical inhomogeneities in the outflows, a subject which has been little investigated so far. In paper I (Corradi et al. 1997a), the results for the bipolar PN IC 4406 were presented, illustrating in detail observations, data reduction and the analysis method. We discuss in the present paper the results for the other 13 PNe. Information about some basic properties of the nebulae can be found in Table 1 of CS95.

Table 2. The selected regions of the nebulae.

| Object | <i>n3</i> | <i>n2</i> | <i>n1</i> | <i>c</i> | <i>p1</i> | <i>p2</i> | <i>p3</i> |
|----------|-------------|--------------|--------------|----------|-------------|-------------|------------|
| NGC 2440 | -40.0 (5.7) | -22.6 (19.7) | -7.8 (9.8) | 0 (5.7) | 7.8 (9.8) | 22.6 (19.7) | 31.2 (5.7) |
| NGC 2818 | | | -12.7 (19.7) | 0 (5.7) | 12.7 (19.7) | 32.4 (19.7) | |
| NGC 2899 | | -29.5 (9.8) | -14.8 (19.7) | 0 (9.8) | 14.8 (19.7) | 29.5 (9.8) | |
| NGC 6072 | | -32.4 (19.7) | -12.7 (19.7) | 0 (5.7) | 12.7 (19.7) | 32.4 (19.7) | |
| NGC 6537 | | | -14.8 (19.7) | 0 (9.8) | 14.8 (19.7) | | |
| He 2-36 | | | -9.8 (9.8) | | 9.8 (9.8) | | |
| He 2-84 | | | | 0 (4.1) | | | |
| He 2-111 | | | -12.7 (19.7) | 0 (5.7) | 12.7 (19.7) | | |
| He 2-114 | | | -7.8 (9.8) | 0 (5.7) | 7.8 (9.8) | | |
| M 1-13 | | | -7.8 (9.8) | 0 (5.7) | 7.8 (9.8) | | |
| M 1-16 | | | | 0 (9.8) | | | |
| M 3-2 | | | | 0 (19.7) | | | |
| Mz 1 | | -32.4 (19.7) | -12.7 (19.7) | 0 (5.7) | 12.7 (19.7) | 32.4 (19.7) | |

For each region, we give the distance (in arcsec) of its middle point from the centre of the nebula, and within brackets the size of the region.

2. Observations

The nebulae were observed on March 1994, at the 1.52m ESO telescope of La Silla, Chile, equipped with a Boller & Chivens spectrograph. On three nights, spectra of the nebulae covering the range from 360 nm to 840 nm were obtained with the long slit of the spectrograph positioned along the major or minor axis of the nebulae. On a fourth night, spectra from 710 nm to 960 nm were secured for some of the objects. With both setups, the reciprocal dispersion was of 0.28 nm pix^{-1} , and the spatial scale $0''.82 \text{ pix}^{-1}$. More details on the detector and gratings used, slit parameters, observing conditions and data reduction are described in paper I. The exposure times and the adopted slit position angles are listed in Table 1.

The long-slit spectrum of each nebula was divided into a number of bins corresponding to spatial regions located at increasing distances from the centre of the object. In each region, average 1-D spectra were extracted by spatial binning. These 1-D spectra usually correspond to the central region of the nebulae, plus few symmetrical zones on each side of the central star. The central regions are referred to as *c*, while regions on the “positive” side (according to the oriented direction defined by the adopted position angle) are named *p1*, *p2*, etc., for increasing distances from the centre, respectively. Analogously, the regions on the “negative” side are called *n1*, *n2*, etc. The exact location of the middle point of each region and its extension are given in Table 2, and visualized in Fig. 1. The line fluxes, normalized to $F_{H\beta}=100$, and the absolute flux of $H\beta$, are listed in Tables 4–16.

3. Physical conditions

The logarithmic extinction constant c_{β} , the electron density $N_e(\text{[SII]})$ and temperatures $T_{[\text{NII}]}$ and $T_{[\text{OIII}]}$, have been computed in each position from the Balmer decrement, the [SII] nebular doublet and the standard auroral to nebular line ratios.

The c_{β} values are listed in Tables 4–16, while densities and temperatures are presented in Tables 17–29.

The computed densities and temperatures are also visualized in Figs. 2–5. The face values of $T_{[\text{OIII}]}$ are typically larger than those of $T_{[\text{NII}]}$, at least in the most central regions of the nebulae, by some 2000–3000 K, the largest difference (about 6000 K) occurring in He 2–111. Various objects result to be quite excited, having $T_{[\text{OIII}]}$ rather above 13000 K throughout the nebulae. They are NGC 2440, NGC 2818, NGC 2899, NGC 6537, He 2–111, and M 3–2. Of these, the latter five reach 16000 K, usually in their central regions. The electron density, as measured from the [SII] doublet, ranges from 50 cm^{-3} (our low density limit) up to 7000 cm^{-3} in the central region of NGC 6537. For the latter nebula, see also the discussion in the following section.

The innermost regions of NGC 6537 has remarkably high electron densities and temperatures. Since data in Table 23 refer to a relatively extended “central” region (the inner 9.8 arcsec), we also extracted a 1-D spectrum corresponding to the innermost $3''.0$, which matches adequately the seeing during observations ($\sim 1''.5$) and some imprecision in the manual guiding. In the core, the [SII] line ratio approaches its high density limit, implying $N_e > 10000 \text{ cm}^{-3}$, and the density for the high ionization regions computed from the [CIII]5518,5538 doublet is of the order of 20000 cm^{-3} or more. Assuming densities in the range $10000\text{--}20000 \text{ cm}^{-3}$, both $T_{[\text{NII}]}$ and $T_{[\text{OIII}]}$ are computed to be between 18500°K and 21000°K . High densities and temperatures were also found by Rowlands et al. (1994), Cuesta et al. (1995), and McKenna et al. (1997). In these works, the spread in both parameters is large, ranging from 17000 cm^{-3} to 30000 cm^{-3} for densities, and from 15000°K to 45000°K for temperature. At least part of these discrepancies are due to the different diagnostic lines used, which are likely to origin in regions with different physical conditions within the core for NGC 6537. In addition, the extent of the central region analysed in the various works is not the same, so that the computed

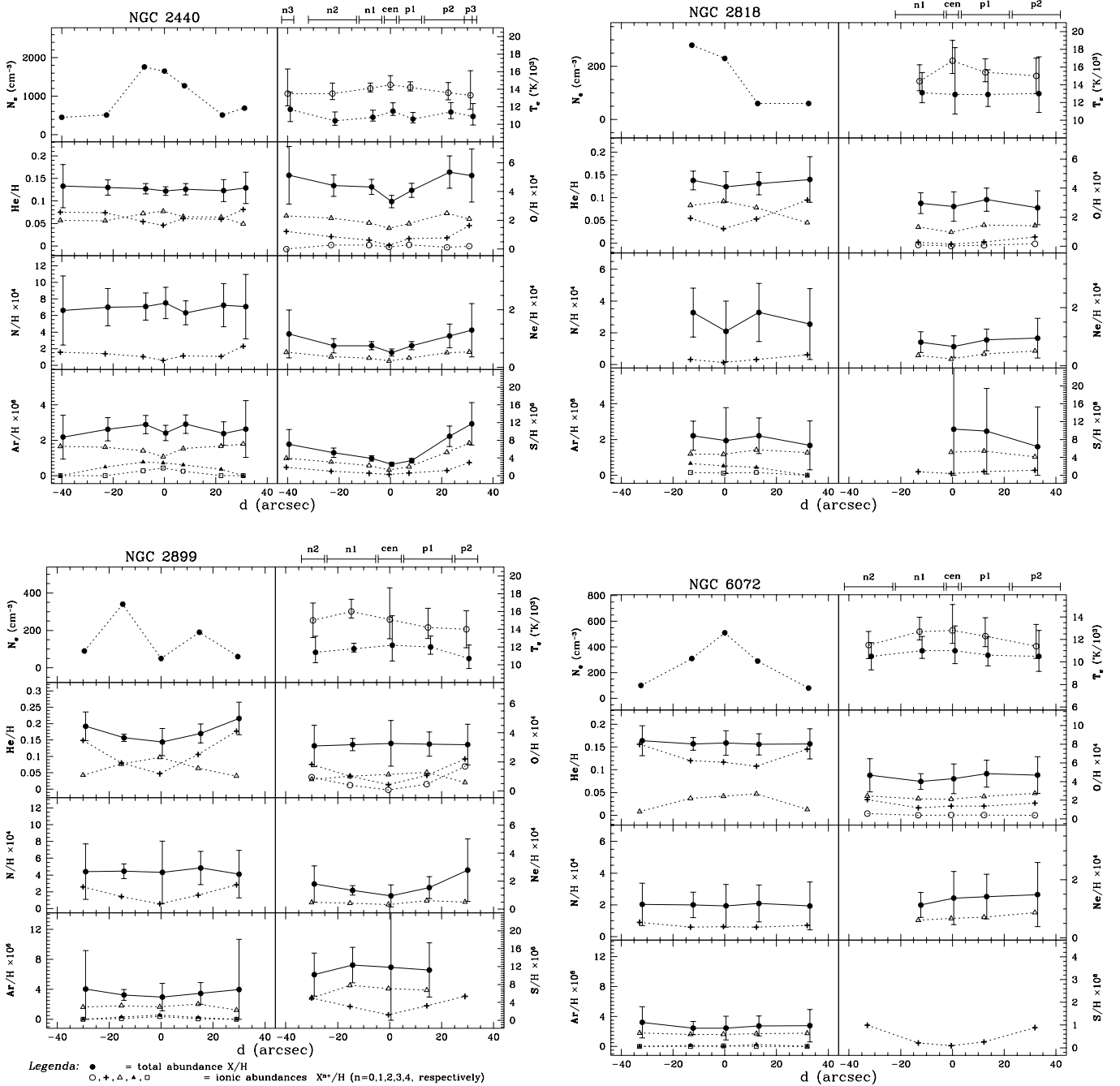


Fig. 2. Density, temperature, and abundance profiles for NGC 2440, NGC 2818, NGC 2899, and NGC 6072. $T_{[NII]}$ and $T_{[OIII]}$ are indicated by filled and open circles, respectively. Symbols are plotted slightly displaced in d in order to avoid overlapping. In the lower panels, ionic and total abundance profiles for He, O, N, Ne, Ar, and S are shown. The explanation of the symbols used is given in the *Legenda* at the bottom of the figure. Above the uppermost right box, the limits of the regions into which the slit was divided are indicated by horizontal “errorbars”.

densities and temperatures are the “averages” within different volumes. As for other PNe with cores with very high densities, see Corradi (1995).

NGC 6537 is known to be a very high excitation object ([SiVI] was detected in NGC 6537 by Ashley and Hyland 1988), with a very hot central star ($T \geq 2 \cdot 10^5$ K, Jacoby & Kaler 1989,

Kaler & Jacoby 1989). Shock excitation is suspected to affect the inner volume of the nebula (Rowlands et al. 1994). Conditions in the high density core of NGC 6537 are therefore quite extreme, and due to the uncertain combination of photo- and shock-ionization the computed physical and chemical parameters in the c region have to be taken with caution.

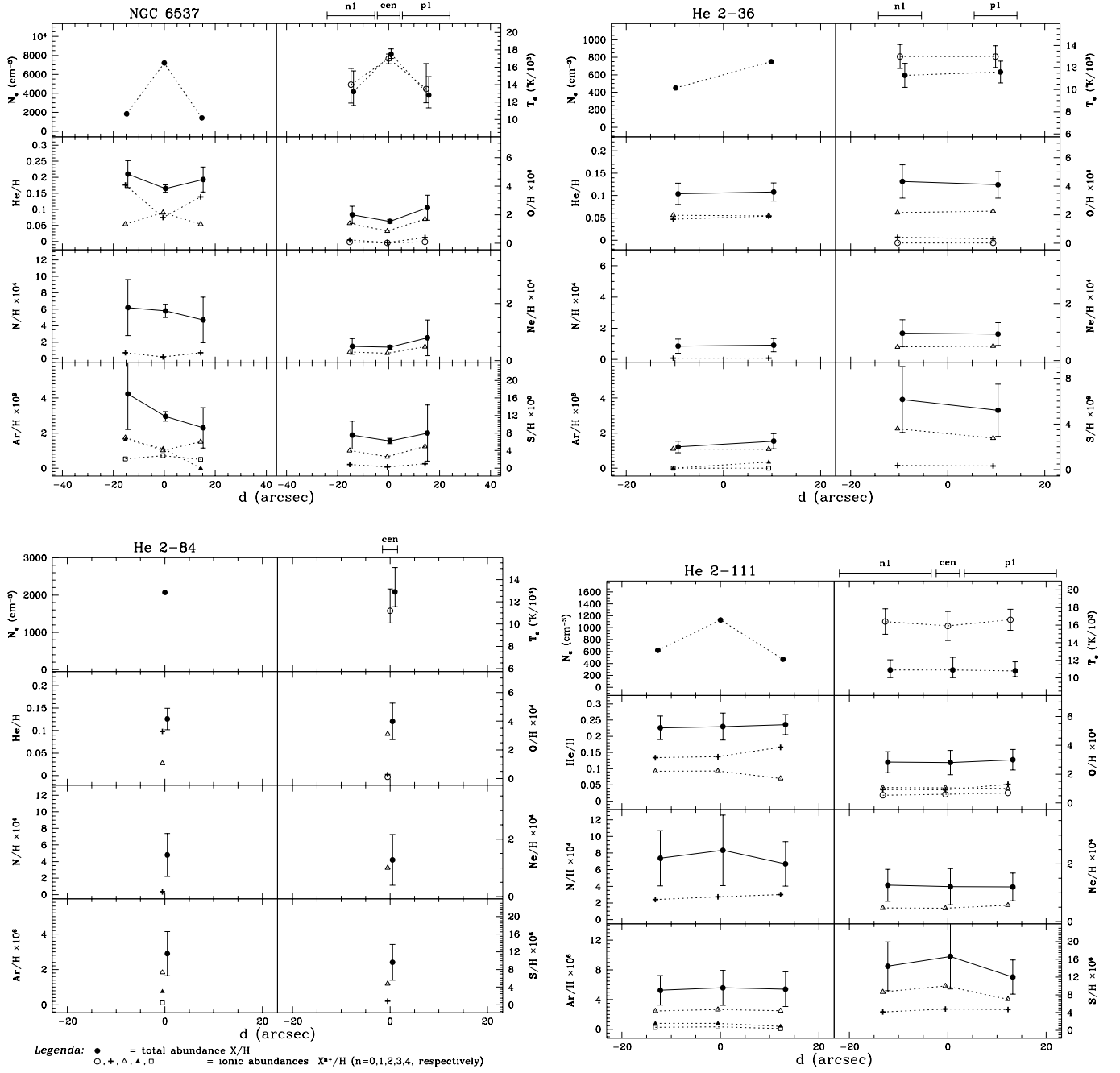


Fig. 3. As for Fig. 2, but for NGC 6537, He 2-36, He 2-84, and He 2-111.

4. Chemical abundances

The ionic and total abundances and their errors were computed from the 1-D spectra for each region as described in paper I. We recall here that a proper scheme, which is essentially the one suggested by Kingsburgh & Barlow (1994, hereafter KB94), was used in adopting temperatures for the lines of different ions. Abundances are listed in Tables 17–29 and plotted in Figs. 2–5 for all the various regions into which nebulae have been divided. As with sulphur, an element whose abundance calculation is particularly uncertain, if the S^{++} ionic abundance cannot be

derived from the [SIII]6312 or [SIII]9069,9531 lines, then the total S/H abundances was not computed.

4.1. The core of NGC 6537

As described in paper I, errors on the ionic abundances were calculated by taking into account both the errors in the line ratios and those on the adopted temperature. The errors on total abundances are obtained by propagating the errors on the mean ionic abundances as well as on the *icf*. Including all that, the final errors on the total abundances are found to be typically of

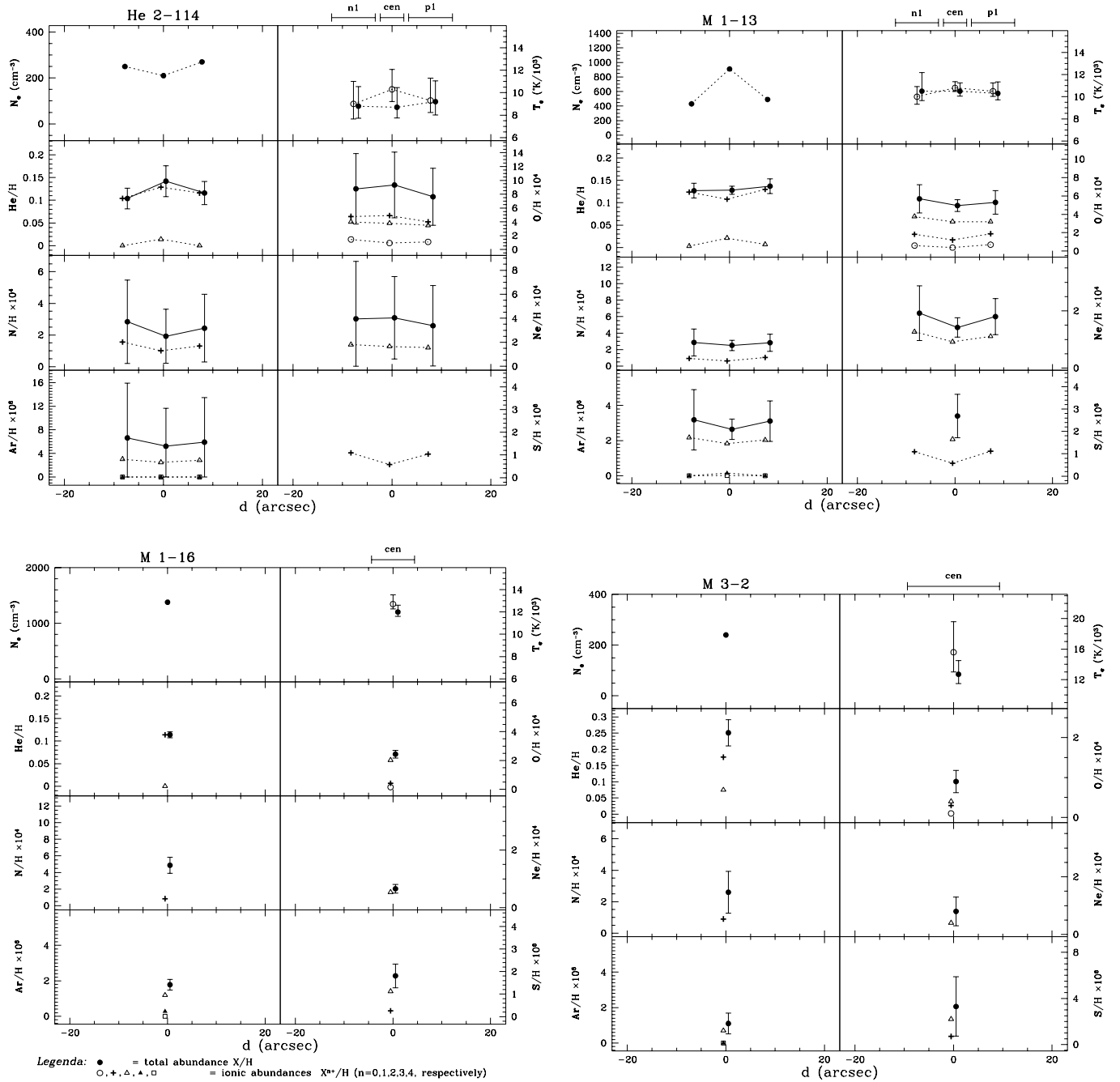


Fig. 4. As for Fig. 2, but for He 2-114, M 1-13, M 1-16, and M 3-2.

10–30% for He (where no *icf* correction is needed, nor the temperature dependence is of importance), and larger for the other elements. As seen in the tables and figures, the largest errors always occur in the outer parts of the nebulae due to limited S/N ratio in these regions. The % errors in the total abundances are indicated within parentheses in Tables 17-29. If errors are larger than 80%, the total abundance is considered to be very uncertain and we indicate it with the symbol “:”. The typical errors associated with the total abundance determinations are as follows.

Oxygen: between 20% and 50%.

Nitrogen: between 20% and 80%, except for He 2-114 and few positions through NGC 2818 and Mz 1 where they are larger.

Neon: between 20% and 80%, excluding NGC 2899, He 2-114, and the outermost position of Mz1.

Argon: errors are similar to those of Ne.

For *sulphur* the information is often incomplete.

The computed errors clearly limit the utility of the present data in highlighting small chemical variations throughout the nebulae. Variations larger than the indicated levels, like those claimed by Guerrero et al. (1995) for the bipolar PN M 1-75, are however expected to be detected.

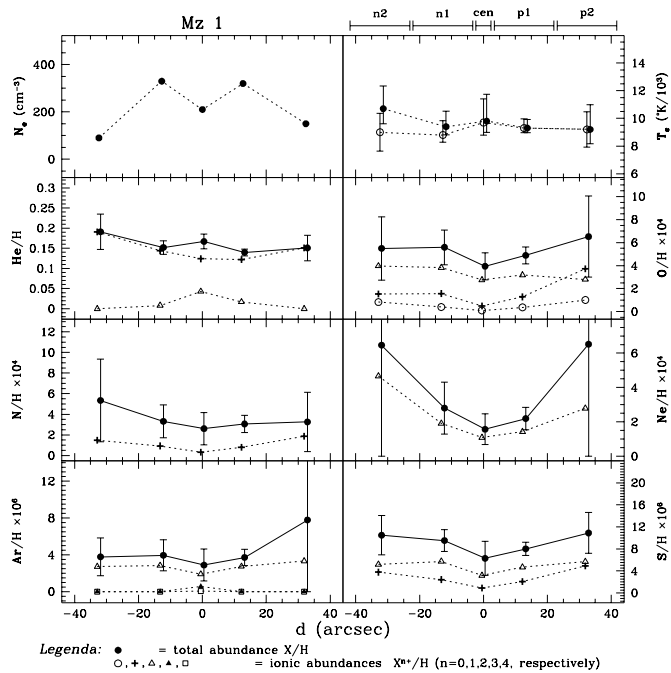


Fig. 5. As for Fig. 2, but for Mz 1.

4.2. Abundances variations through the nebulae

Inspection of Figs. 2–5 and 6 shows that no variations of the He, O, and N abundances are detected through the nebulae within our present errors. The case of M 1–75 (Guerrero et al. 1995), where a significant decrease of the N/O in the core of the nebula was detected, seems therefore to remain an isolated one.

We recall here that the ionic N^+/O^+ ratio is usually taken as a measure of the total N/O ratio, because of the similar ionization potentials of the relevant species (but caution has to be taken owing to the possible importance of charge–exchange reactions with hydrogen; cf. Osterbrock, 1989). The N^+/O^+ profiles of all nebulae are presented in Fig. 6. In the figure, no changes in the N^+/O^+ ratio are observed throughout the nebulae, within the computed errors which are often of the order of 30%, certainly smaller than those which would have been deduced by combining the errors in the N and O total abundances. A possible variation in N^+/O^+ is indicated only at the centre of NGC 2440, where it results to be by a factor of 1.4 larger than in the rest of the nebula. This variation is however just at the limit of the errorbars, and we consider it as tentative. Note, however, that the same apparent central increase of the N/O ratio has been found by Guerrero (1995).

As for Ne, Ar, and S, the situation is different in the following sense. As noted in paper I for IC 4406, clear trends are observed in the abundance profiles of these elements, although usually within the computed errors. If we consider the face values in 5 nebulae of our sample in which the chemical information is extended to their faint outer regions (IC 4406, NGC 2440, NGC 2899, NGC 6072, and Mz 1), we find that: *i*) the abundance of the three elements remains practically constant throughout the nebula in NGC 6072; *ii*) in the other four nebu-

lae, the abundances of neon, argon, and sulphur increase from the centre to the border by factors between 1.3 and 5, depending on the specific element and nebula. For Ne, the centre–border variations amount to a factor between 2.5 and 4; for Ar, between 1.3 and 2.5; and for S, between 1.7 and 5 (except for NGC 2899, where S is constant).

As discussed in paper I, this systematic effect may have to do with the use of an improper ionization correction scheme (KB94), when going to the outer parts of the nebula. This kind of effect is predicted by Alexander and Balick (1994) for long-slit observations of spherical PNe. On the other hand, from the various nebulae studied in the present paper we confirm the result found in paper I for IC 4406: nitrogen, which has the largest icf, is not affected by this problem. The matter deserves then some explanation that we cannot offer at present. In any case the systematic effect, which is noticeable for Ne, Ar and S, is at present an additional limitation in the search for abundance variations of these elements across the nebulae.

We conclude that no abundances changes are detected across the objects studied in the present work to within variations of, essentially, 30%, 50%, and 80% for He, O and N, respectively, and to within larger intervals for Ne, Ar, and S depending on the element and nebula. No variations are either found, within some 30%, for the N^+/O^+ ratio, which is commonly taken as a measure of the total N/O abundance ratio. This refers to the five nebulae observed in 5–7 spatial positions, up to their faint outer regions. For the objects observed in less positions, the precision in the abundance determinations is generally higher (see Tables 17–29).

4.3. Average abundances

Considering that no clear evidence is found for abundance variations throughout the nebulae, average abundances were computed by weighting the determinations in the different positions with both their errors and a “mass” factor (proportional to the square root of the total $H\beta$ flux from that region). For NGC 6537, following the remarks in sect. 4.1, the central region *c* was not given a larger weight than the surrounding ones. Average abundances are listed in Table 3.

4.4. $[NII]/H\alpha$ line ratios vs. N/O abundances

It has been sometimes questioned whether the high $([NII]6548+6583)/H\alpha$ line ratios measured in bipolar PNe, and in particular in their lobes, are unequivocal signatures of nitrogen enrichment. In Fig. 7 we plot the observed $[NII]/H\alpha$ line ratios vs. the average N/O abundances. For each nebula in our sample, the $[NII]/H\alpha$ ratio *integrated* all over the slit (simulating the case of a very distant nebula which is not spatially resolved) is indicated by a filled circle, while dotted lines give the range of line ratios showed in the various positions along the slit. For some objects, measurements have been extended to extremely faint regions, which were not considered in our chemical analysis since only the $[NII]$ and $H\alpha$ emission could be measured over the entire observed spectral range. In Fig. 7, we also plot

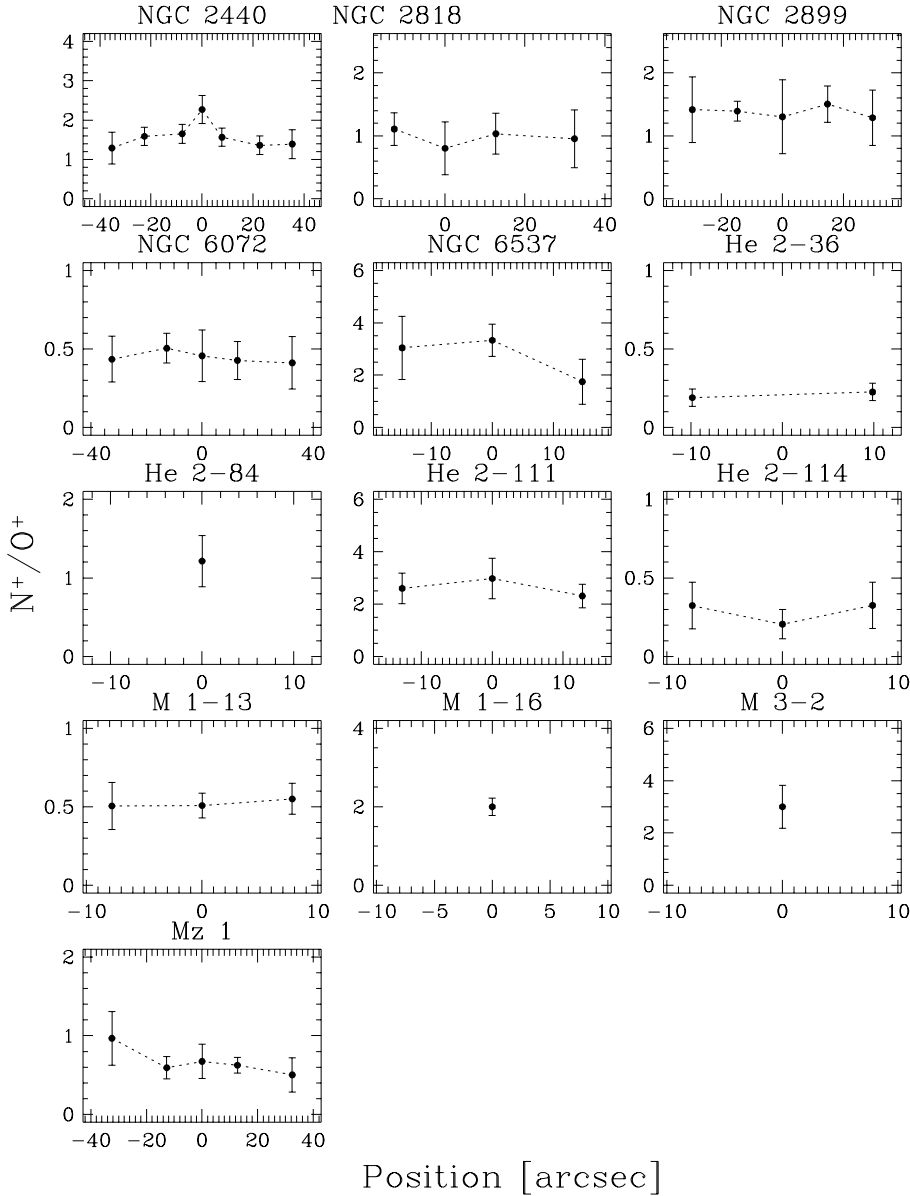


Fig. 6. N^+/O^+ profiles of the nebulae.

with empty circles data for the 32 nebulae in KB94 for which the complete information ($H\alpha$ and $[NII]$ fluxes, N/O abundance) is available, excluding those objects which are already included in our sample. It has to be noted that most of these 32 nebulae are not bipolar.

A trend of increasing N/O abundance with the $[NII]/H\alpha$ line ratios is evident, but scatter is very large. In addition, for each object in our sample the internal variations of $[NII]/H\alpha$ are also quite large (≤ 0.8 dex), while the N/O ratio was shown to be approximately constant throughout the nebulae. Nevertheless, the correlation in Fig. 7 can be used, for instance, to pick up nebulae with very high N/O abundances (and thus likely massive progenitors) by simply measuring their integrated $[NII]/H\alpha$ line ratios (note that $[NII]/H\alpha \geq 3$ always points to a $N/O \geq 1$). This can be valuable for statistical purposes, or for selecting specific classes of highly over- or under-abundant objects in spectroscopic and narrowband imaging surveys of PNe.

4.5. Comparison with previous studies

Previous abundances determinations exist for 9 of the 13 PNe discussed in this paper (Perinotto 1991, Koppen et al. 1991, KB94, Baessgen et al. 1995, and Guerrero 1995 for NGC 2440; Perinotto 1991, Guerrero 1995, and De Freitas-Pacheco et al. 1992 for NGC 2818; Lopez et al. 1991 and KB94 for NGC 2899; Perinotto 1991 and Perinotto et al. 1994 for NGC 6537; Gutierrez-Moreno et al. 1994, De Freitas-Pacheco et al. 1992, and KB94 for He 2-111; Perinotto 1991 and KB94 for M 1-13; Kaler et al. 1996 for M 1-16; Koppen et al. 1991 for M 3-2; Perinotto et al. 1994 for Mz 1). Note that the work by Perinotto (1991) is not an original work, but a critical compilation based upon original measurements by other authors. For determinations obtained before 1990, we have just referred to that extensive compilation, in which the reader can find the references to the original papers. For NGC 6072, He 2-36, He 2-84, and He 2-114 we did not find any previous chemical study. It has

Table 3. Average abundances.

| Object | He/H | O/H ($\times 10^4$) | N/H ($\times 10^4$) | Ne/H ($\times 10^4$) | Ar/H ($\times 10^6$) | S/H ($\times 10^6$) | N ⁺ /O ⁺ |
|------------------------------|-------------|--------------------------|--------------------------|---------------------------|---------------------------|--------------------------|--------------------------------|
| NGC 2440 | 0.124±0.003 | 3.8±0.6 | 7.0±0.6 | 0.6±0.2 | 2.6±0.3 | 3.1±1.0 | 1.70±0.33 |
| NGC 2818 | 0.134±0.006 | 3.0±0.2 | 3.0±0.6 | 0.8±0.1 | 2.2±0.2 | 8.7±1.4 | 1.04±0.13 |
| NGC 2899 | 0.159±0.016 | 3.2±0.1 | 4.5±0.3 | 1.4±0.3 | 3.3±0.2 | 11.8±1.1 | 1.41±0.08 |
| NGC 6072 | 0.157±0.002 | 4.3±0.4 | 2.0±0.1 | 1.2±0.2 | 2.6±0.3 | | 0.47±0.04 |
| NGC 6537 | 0.189±0.023 | 2.0±0.5 | 5.6±0.8 | 0.6±0.2 | 3.2±1.0 | 7.2±0.9 | 2.71±0.84 |
| He 2-36 | 0.106±0.002 | 4.2±0.2 | 0.9±0.1 | 0.9±0.1 | 1.3±0.2 | 5.5±0.7 | 0.21±0.02 |
| He 2-84 | 0.126±0.024 | 4.0±1.3 | 4.8±2.6 | 1.3±0.9 | 2.9±1.2 | 9.6±4.0 | 1.21±0.33 |
| He 2-111 | 0.231±0.006 | 2.9±0.1 | 7.2±0.8 | 1.2±0.1 | 5.4±0.2 | 13±2 | 2.49±0.31 |
| He 2-114 | 0.115±0.017 | 8.4±0.9 | 2.3±0.5 | 3.7±0.4 | 5.8±0.7 | | 0.26±0.08 |
| M 1-13 | 0.129±0.005 | 5.1±0.4 | 2.6±0.2 | 1.5±0.3 | 2.7±0.3 | 2.7±1.0 | 0.52±0.03 |
| M 1-16 | 0.114±0.006 | 2.4±0.3 | 4.9±1.0 | 0.7±0.2 | 1.8±0.3 | 1.8±0.5 | 2.00±0.22 |
| M 3-2 | 0.251±0.040 | 0.9±0.4 | 2.6±1.3 | 0.8±0.5 | 1.1±0.6 | 3.3±2.5 | 2.97±1.12 |
| Mz 1 | 0.146±0.015 | 4.8±0.7 | 3.0±0.4 | 2.1±0.6 | 3.6±0.5 | 8.3±1.4 | 0.62±0.07 |
| IC 4406 [†] | 0.126±0.015 | 5.6±1.3 | 2.0±0.9 | 1.7±0.7 | 3.2±1.1 | | 0.36±0.01 |
| PN G321.6+0.2.2 [‡] | 0.147±0.029 | 5.7±2.8 | 17±12 | | 5.2±1.3 | 27±14 | 2.95±1.73 |
| <i>Average</i> | 0.150±0.043 | 4.0±1.8 | 4.6±3.9 | 1.3±0.8 | 3.1±1.4 | 8.5±7.0 | 1.39±1.02 |

[†]paper I; [‡]Corradi et al. 1997b

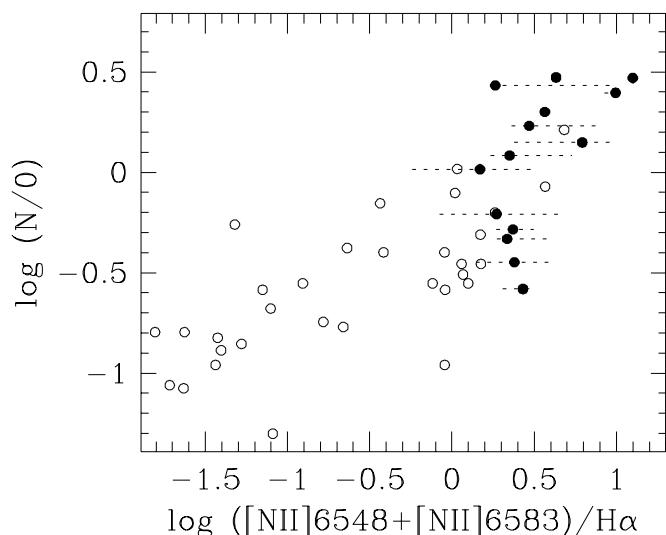


Fig. 7. The correlation between the [NII]/H α line ratio and the N/O abundance. Dots are the ([NII]6548+6583)/H α ratio for each nebula *integrated* all over the slit length, while the dotted lines give the range of line ratios showed by each object when fluxes are measured *locally*, i.e. in the spatial resolution elements along the slit. Empty circle represent the data for 32 PNe from KB94.

also to be remembered that all the studies mentioned above, except for the one by Guerrero (1995) and Perinotto et al. (1994), do not contain spatially resolved chemical information through the nebulae.

As expected considering the different quality of the observations and analysis methods, several discrepancies between the determinations of the various authors are found. Since a detailed one-by-one comparison would result quite dispersive and not really instructive, we only mention some individual pecu-

liarities which we consider to be noteworthy. As noted in paper I for IC 4406, also in the cases of NGC 2818 and He 2-111 the O, N, and Ar abundances from de Freitas-Pacheco et al. (1992) are by a factor between two and four systematically higher than the determinations from all other authors (and, for He 2-111, their He abundance is by a factor 1.6 smaller than ours). In the two cases where the comparison is possible, a systematic difference also appears between our He abundance and those of Koppen et al. (1991), their value being lower by up to a factor 1.5. Generally, excluding some exceptions, the determinations from the different authors agree with our results within some 20% for He, and some 40–50% for O, N, and Ne. Ar, and S present larger discrepancies.

5. Discussion

About 60 bipolar PNe are known in the Galaxy (CS95, Manchado et al. 1996, Corradi et al. 1997b). The present sample of 15 objects (including IC 4406, paper I, and PN G321.6+0.2.2, Corradi et al. 1997b) therefore represents a significant fraction (25%) of this morphological class of PNe, and some general considerations can be drawn.

In Fig. 8 we plot the abundances of the 15 bipolar PNe in the usual log(N/O) vs. He/H diagram (N⁺/O⁺ is used here instead of N/O because errors are lower, but all the following conclusions would still hold if we use the ratio between the total N and O abundances). As noticed by Peimbert (1978), and remarked by CS95, the great majority of objects in this morphological class are type I PNe, i.e. He and/or N rich. It has to be noticed that the present sample includes four objects which are possibly the PNe in Galaxy with the highest He and/or N/O abundances known up to date: PN G321.6+0.2.2, NGC 6537, He 2-111, M 3-2, to which M 1-75 (Guerrero et al. 1995) has

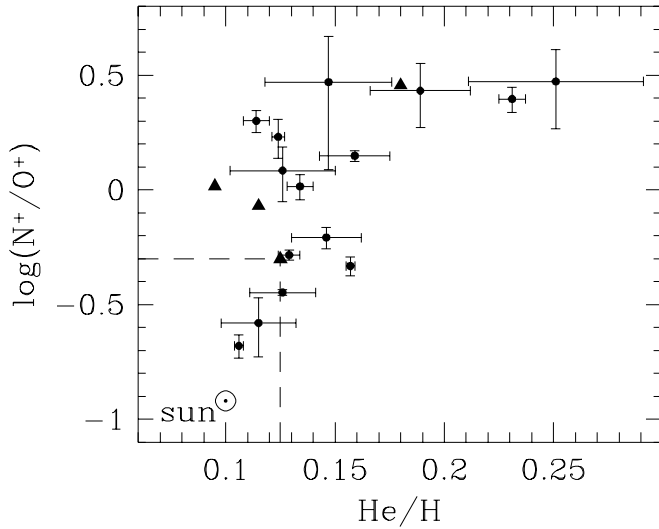


Fig. 8. $\log(N^+/O^+)$ vs. He/H diagram for the 15 bipolar PNe (dots with errorbars). The three helium-rich nebulae on the top of the diagram are, from right to left, M 3–2, He 2-111, and NGC 6537. Triangles are data for the bipolar PN M 1–75 (Guerrero et al. 1995), MyCn 18, M 1–8, and M 3–3 (KB94). The region at the top-right of the dashed lines is the locus of type I PNe (Peimbert & Torres-Peimbert 1983).

to be added. The points in Fig. 8 seem to be grouped in a sequence of increasing N/O for an almost constant He, up to an upper limit of $\log(N/O) \sim 0.5$ at which the points start to be displaced toward very high He/H (up to 0.25!) without any further increase of the N/O ratio. The sequence of increasing N/O for bipolar PNe is qualitatively reproduced by the models of Renzini & Voli (1981) for quite massive progenitors ($M_i = 3-5 M_\odot$), considering an efficient H-burning at the base of the convective envelope. No theoretical models exist, however, which are able to reproduce He overabundances as large as those shown by NGC 6537, He 2-111, and M 3–2 (Marigo et al. 1996, and 1997, private communication).

The possible Ne enrichment of bipolar PNe suggested by CS95 remains controversial. The mean Ne/O abundances ratio of the present sample (0.33 ± 0.15) is higher than that of elliptical PNe in CS95 (0.22 ± 0.07). On the other hand, the evidence of a Ne enrichment is marginal when the Ne/H ratio is considered ($1.3 \pm 0.8 \times 10^{-4}$ for our sample vs. 1.0 ± 0.5 for the elliptical PNe in CS95). Also when comparing with the sample of non-type I in KB94 (average Ne/H = 1.3 ± 0.5), no evidence is found of a Ne enrichment of our sample of bipolar PNe. This is certainly a point which deserves further study, since the Ne enrichment could be the signature of efficient third dredge-up in the most massive PNe progenitors (Gallino et al. 1990).

In the present sample, there are 2 bipolar objects (He 2–36, and He 2–114) which are not type I PNe. These nebulae appear to have a “moderate” bipolar shape, since their equatorial waist is not very pronounced. In fact, if one compares the sequence of increasing N/O in Fig. 8, with the images of the corresponding nebulae in Fig. 1 (see also Fig. 2 in CS95 for the full image of He 2-111), making use of Table 3, an overall correlation is found between the N/O abundance and the “degree of

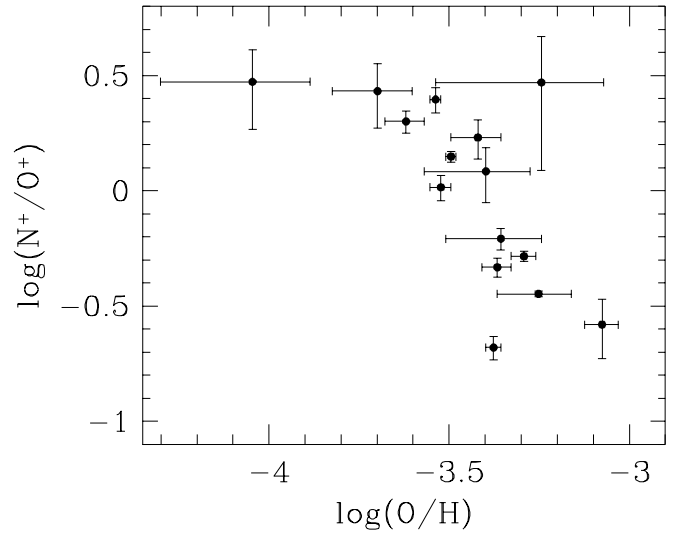


Fig. 9. $\log(N^+/O^+)$ vs. $\log(O/H)$ diagram for the 15 bipolar nebulae.

bipolarity”, estimated as the ratio between the maximum length and the minimum width of the objects, or alternatively, between their maximum width (measured in the lobes) to their minimum width (in the equatorial waist). According to Mellema (1997), bipolar PNe are more likely to develop from large mass progenitors, because the fast post-AGB evolution of their central stars avoids that the ionization front modifies the original density distribution, as instead occurs in low-mass progenitors preventing the formation of a marked bipolar morphology even if the initial conditions (AGB mass loss geometry) were favorable. According to these models, the present data further supports the conclusion that the PNe with high N/O and He abundances are produced by massive progenitors.

5.1. Other correlations between elements

The $\log(N^+/O^+)$ vs. $\log(O/H)$ plot for our 15 bipolar PNe is presented in Fig. 9. Up to the value $\log(N^+/O^+) = 0.2$, there is some marginal evidence for a possible existence of an anti-correlation between $\log(N/O)$ and $\log(O/H)$, which relies on the position of the 2–3 points with the lowest N/O. We conservatively conclude that our data do not support the existence of such a correlation for these values of N^+/O^+ . This is in agreement with the results of KB94. On the other hand, for $\log(N^+/O^+) > 0.2$ we find that nebulae tend to have lower oxygen abundances (only one object does not follow this tendency, but has very large errors). Note that KB94 in their similar diagram (their Fig. 5), have only two points above $\log(N/O) > 0.2$. It is certainly important to obtain further confirmation of the mentioned anticorrelation, considering the discrepant results of the different authors (see the extensive discussion in KB94). Nevertheless, we think that our data support, with some caution, the existence of such an anticorrelation for objects with $\log(N^+/O^+) > 0.2$. This would imply that, at least for the highest mass progenitors, a significant amount of nitrogen is formed at expenses of oxygen via a quite efficient ON-cycle.

Finally, we confirm the conclusion by KB94 that the Ar abundance does not correlate with the N/O ratio, at variance with the results from de Freitas–Pacheco et al. (1992).

6. Summary and conclusions

We have presented a spectroscopic study of 13 bipolar PNe in which chemical information has been derived in different regions of the nebulae. While the present data do not allow to test for abundances variations through the nebulae smaller than, at best, some 10–20% for helium, 10–40% for oxygen, and larger for the other elements (see Sect. 4), they are still very useful in order to highlight large abundances variations as the ones claimed for other objects by some authors (Balick et al. 1994, Guerrero et al. 1995), as well as to derive accurate mean abundances for the objects, which can be obtained by averaging determinations obtained in regions of the objects with different ionization/excitation conditions.

Long-slit spectra obtained with larger class telescopes than the one used in the present study would be necessary in order to obtain high S/N in the very faint region of these nebulae, and minimize everywhere the errors due to the uncertainties in the flux measurements.

The results of this study are summarized below.

- Within the present errors, the He, O, and N abundances are constant throughout all the studied nebulae, with the possible exception of NGC 2440 where a tentative increase of a factor 1.4 of the N/O abundance ratio has been detected in the innermost region. Further work is however needed to confirm it.

- The Ne, Ar, and S abundances show systematic increases toward the outer regions of the nebulae. Although they are within the errors, these trends are systematic. They might be ascribed to inaccuracies in the *icfs*, as predicted by Alexander & Balick (1997). Note, however, that the corresponding apparent increase of the N abundance predicted by Alexander & Balick (1997) is generally *not* observed in our sample.

- The present sample contains some of the Galactic PNe with the highest He and N/O abundances known up to date. In particular, the highest He abundances cannot be reproduced by any current models of AGB evolution.

- The question of the possible Ne overabundance of the class of bipolar PNe, as compared to the general sample of Galactic PNe, remains controversial.

- A positive correlation is found between the observed $([\text{NII}]6548+6583)/\text{H}\alpha$ line ratio and the N/O abundance. Due to the large scatter in the correlation, its use is limited to statistical purposes, or as a tool to select objects with likely high N abundances in large spectroscopic or narrowband imaging databases.

- Oxygen depletion is suggested for the PNe with the highest N/O abundances, which is likely to be the consequence of efficient ON-cycle process in their high mass progenitors.

- High electron densities and temperatures are measured in the core of NGC 6537.

Acknowledgements. We thank Hugo Schwarz and Jean–François Claeskens for taking the observations. We also acknowledge useful criticism and suggestions by an anonymous referee. The work of RLMLC has been supported by a grant of the DGYCIT PB94–1108.

References

- Alexander, J., Balick, B.: 1997, AJ 114, 713
 Ashley, M.C.B., Hyland, A.R.: 1988, ApJ 331, 538
 Baessgen, M., Diesch, C., Grewing, M.: 1995, A&A 297, 828
 Balick, B.: 1987, AJ 94, 671
 Balick, B., Perinotto, M., Maccioni, A., Terzian, Y., Hajian, A.: 1994, ApJ 424, 800
 Corradi, R.L.M.: 1995, MNRAS 276, 521
 Corradi, R.L.M., Schwarz, H.E.: 1995, A&A 293, 871 (**CS95**)
 Corradi, R.L.M., Perinotto, M., Schwarz, H.E., Claeskens, J.–F.: 1997a, A&A 322, 975 (**paper I**)
 Corradi, R.L.M., Villaver, E., Mampaso, A., Perinotto, M.: 1997b, A&A 324, 276
 Cuesta, L., Phillips, J.P., Mampaso, A.: 1995, A&A 304, 475
 Curtis, H.B.: 1918, Lick Obs. Publ. XIII, p. 57
 de Freitas Pacheco, J.A., Maciel, W.J., Costa, R.D.D.: 1992, A&A 261, 579
 Gallino, R., Busso, M., Picchio, G., Raiteri, C.M.: 1990, Nature 348, 298
 Guerrero, M.A.: 1995, Thesis, University of La Laguna, Tenerife, Spain
 Guerrero, M.A., Stanghellini, L., Machado, A.: 1995, ApJ 444, L49
 Gutierrez-Moreno A., Moreno H., Cortes, G.: 1994, PASP 106, 869
 Jacoby, G.H., Kaler, J.B.: 1989, AJ 98, 1662
 Kaler, J.B., Jacoby, G.H.: 1989, ApJ 345, 871
 Kaler, J.B., Kwitter, K.B., Shaw, R.A., Browning, L.: 1996, PASP 108, 980
 Kingsburgh, R.L., Barlow, M.J.: 1994, MNRAS 271, 257 (**KB94**)
 Koppen, J., Acker, A., Stenholm, B.: 1991, A&A 248, 197
 Lopez, J.A., Falcon, L.H., Ruiz, M.T., Roth, M.: 1991, A&A 241, 526
 Machado, A., Guerrero, M.A., Stanghellini, L., Serra-Ricart, M.: 1996, ‘The IAC Morphological Survey of Northern Galactic PNe’, IAC, La Laguna
 Marigo, P., Bressan, A., Chiosi, C.: 1996, A&A, 313, 545
 McKenna, F.C., Keenan, F.P., Kaler, J.B., Wickstead, A.W., Bell, K.L., Aggarwal, K.M.: 1997, PASP 108, 610
 Mellema, G.: 1997, A&A 312, L29
 Osterbrock, D.E.: 1989, ‘Astrophysics of Gaseous Nebulae and Active Galactic Nuclei’, University Science Books, Mill Valley, California.
 Peimbert, M.: 1978, in Planetary Nebulae, IAU Symp. n.76, , ed. Y. Terzian, Dordrecht: Reidel, p. 215
 Peimbert, M., Torres–Peimbert, S.: 1983, in Planetary nebulae, IAU Symp.n.103, Flower ed., p.233
 Perinotto, M.: 1991, ApJS 76, 687
 Perinotto, M., Purgathofer, A., Pasquali, A., Patriarchi, P.: 1994, A&AS 107, 481
 Renzini, A., Voli, M.: 1981, A&A 94, 175
 Rowlands, N., Houck, J.R., Herter, T.: 1994, ApJ 427, 867
 Schwarz, H.E., Corradi, R.L.M., Stanghellini, L.: 1993, in Planetary nebulae, IAU Symp. N.155, eds. Weinberger & Acker, p. 214